Energy 147 (2018) 490–503

Contents lists available at ScienceDirect

Energy

journal homepage: www.elsevier.com/locate/energy

Multi-objective optimization of hybrid CSP+PV system using genetic algorithm

Allan R. Starke [a, *], José M. Cardemil [b], Rodrigo Escobar [c], Sergio Colle [a]

[a] LEPTEN-Laboratory of Energy Conversion Engineering and Energy Technology, Department of Mechanical Engineering, Federal University of Santa Catarina (UFSC), Florianópolis, Brazil
[b] Mechanical Engineering Department, Universidad de Chile, Beauchef 851, Santiago, Chile
[c] Centro de Energía, Centro del Desierto de Atacama, Pontificia Universidad Católica de Chile, Santiago, Chile

ARTICLE INFO

Article history:
Received 19 June 2017
Received in revised form
6 November 2017
Accepted 22 December 2017
Available online 12 January 2018

Keywords:
CSP+PV hybrid
Baseload electricity
Solar energy
Multi-objective optimization

ABSTRACT

Renewable energy has experienced a significant growth on its rate of deployment as a clean and competitive alternative for conventional power sources. The reduction on the installation costs for PV systems has converted this technology into a relevant player regarding the electricity matrix. However, a larger penetration of PV systems is restricted to the availability of affordable technological options for storage. The integration of thermal energy storage to CSP systems is, on the other hand, straightforward through technologies already available in the market. Hence, the hybridization of CSP and PV systems has the potential for reducing operational and installation costs, as well as increasing significantly the capacity factor of solar power plants. The present study describes a methodology for design and sizing such hybrid plants, by implementing a transient simulation model, coupled to an evolutionary optimization algorithm, allowing to address the trade off between costs and capacity factor. The simulation model is applied to a case study considering the characteristics of a location in northern Chile. The results are presented in terms of the Pareto Frontiers that summarizes the compromise between the economic performance and the capacity factor of the plant. It is observed that the capacity factor achieves values higher that 85%, and the LCOE is lower than those observed for stand alone CSP plants. The methodology developed constitutes a useful tool for decision makers, who can assess the performance of the hybrid plant based in a detailed transient simulation and selecting the best configuration according to market constraints or its willingness for achieving certain level of capacity factor.

1. Introduction

The growing awareness regarding global warming has encouraged the scientific community to carry out research on sustainable substitutes for the fossil fuels, which utilization presents environmental impacts and is subject to resource depletion due to its non-renewable feature. In that context, during the last decade renewable energy technologies have been deployed at a high rate and show potential to become a relevant players on electricity supply, before 2030 [1]. Indeed, the installed capacity has grown significantly for wind and solar technologies, where the biggest player regarding deployment of new renewable projects is China, but significant projects have been deployed also at the European Union (wind); India and USA (PV); Africa and Latin America (hydro) [1].

Among the renewable technologies, PV systems stands out with a meaningful growth on its installed capacity and daytime penetration, propelled by its significant cost reduction. Despite the effort devoted to improvements on the grid and demand response infrastructure, the potential contribution of PV to the electricity supply is limited by the availability of affordable technological options for energy storage [2]. Indeed, several authors have reported that is unlikely for PV technologies to supply a share of world's electricity matrix larger than 10%, without any striking change on costs for electricity storage [3,4]. Solar and wind resources have a complementary nature and can be operated as a hybrid renewable energy system (HRES) [5,6], however both present an intermittent availability. Due to that feature, such sources demands reliable energy storage solutions in order to improve their operational performance and reliability (mis-balances among other

* Corresponding author.
E-mail address: allan.starke@lepten.ufsc.br (A.R. Starke).

https://doi.org/10.1016/j.energy.2017.12.116
0360-5442/

issues in grid management). One alternative that has been analyzed is the hybridization with other energy sources, as suggested in Ref. [7]. Among the options for hybridization, one of the most promising schemes is the CSP + PV, which combines the low installation cost of PV, with the storage of CSP, allowing to reduce the LCOE, as well as increase the capacity factor.

The performance of hybrid CSP + PV plants has been analyzed by several authors [8–12], who performed an optimization procedures, minimizing the LCOE and considering the capacity factor as a constrain. Green et al. [8] analyzed the effect of PV tilt angle, optimizing it in terms of the capacity factor. Their conclusions state that at higher tilt angles, the system achieves an annual capacity factor higher than 80%, reducing the seasonality effects. Platzer [9] shows that hybrid CSP + PV plants could achieve capacity factors above 70% and provide lower energy costs than CSP-only plants, by reducing the size of the storage and solar field size. Petrollese and Cocco [10] studied a hybrid CSP + PV plant in which the CSP section consist of linear Fresnel collectors using thermal oil as heat transfer fluid, a two-tank direct TES system and an Organic Rankine Cycle (ORC). For the PV section, the PV array is considered as coupled to a battery bank for electrochemical storage. The authors showed that the hybrid scheme becomes highly cost-effective for base-load production. Cocco et al. [11] determined the improvements on dispatchability using a hybrid CSP + CPV (Concentrating Photovoltaic) plants. The authors showed the advantages of using an integrated management strategy to satisfy a constant power output profile. Optimization of the CSP and CPV power share leads to an effective use of the dispatch capabilities of the CSP plant, owe to the operation of TES, while the CPV plant is fully exploited during the hours of high solar radiation. In a previously publication of our group, Starke et al. [12] presented a power generation and economic analysis of two hybrid CSP + PV plant models, considering a range of plant capacities based on parabolic trough or central receiver plants, combined with a PV field. The authors optimized the plants, minimizing the LCOE and considering a capacity factor higher than 80% as a constraint. In that context, solar multiple, storage size and PV tilt angle were considered as decision variables. The results showed that CSP + PV hybrid schemes increases the domain of solutions with a high capacity factor, so a plant with a smaller CSP solar field can achieve capacity factors of 80% or higher. Therefore, the main advantage of the hybridization of a CSP plant with a PV array is reducing the size of the CSP solar field, while maintaining a high capacity factor and lowering the LCOE.

Within the studies that analyze the performance of CSP + PV systems, it results clear the trade-off between LCOE and capacity factor, which constitutes two objective functions, rather than a constraint. In that regard, the present article describes the use of multi-objective optimization for designing such systems. Multi-objective optimization has been extensively used for the design and optimization of thermal systems [13–17]. Lazzaretto and Toffolo [13] demonstrated the use of an evolutionary algorithm to optimize and design a thermal system using energy, economy, and environmental attributes as objective functions. Magnier and Haghighat [14] presented a methodology to optimize the thermal comfort and energy consumption in a residential house. Since optimizing a building is a time-consuming process, the authors used an artificial neural network approach (ANN) to characterize the thermal behavior of the building, and a multi-objective genetic algorithm to perform the optimization procedure. The results show a significant reduction in energy consumption and an improvement in thermal comfort, revealing several potential designs and a wide degree of compromise between thermal comfort and energy consumption. Ahmadi et al. [15] performed a multi-objective optimization procedure for designing a combined cycle power plant considering exergetic, economic, and environmental factors. They showed that the optimization procedure for a combined cycle power plant requires a practical and comprehensive approach that enables the utilization of multi-objective optimization. Asadi et al. [16] described a multi-objective optimization scheme for retrofitting a building. The methodology consisted of optimizing the retrofit cost, energy savings, and thermal comfort of a residential building. The results demonstrated the enforceability of providing decision support in an actual configuration, allowing simultaneous consideration of all available combinations of retrofit actions. Li et al. [17] presented a multi-objective optimization of solar-dish Brayton system driven by a hybrid system composed of a fossil fuel burner and solar energy collectors. The authors considered the maximum power output, thermal efficiency and ecological performance as objective functions and the NSGA-II algorithm was used for the optimization process. Regarding the solution selection three decision making approaches were compared: Shannon Entropy, LINMAP and TOPSIS.

As described above, the technical viability, and competitiveness of hybridizing CSP and PV plants have been addressed by several authors. The performance of these plants and the optimal design considering only the minimization of the plant LCOE have been found. However, the effect of the design parameters – size of the solar field, thermal storage capacity, PV tilt angle and PV power ratio (ratio between PV installed capacity and CSP nameplate capacity) – on the performance figure of merits – capacity factor and Total investment – has not been studied yet. In fact, simultaneously optimizing the most important figure of merits of a CSP + PV plant, and determining the existing trade-offs between the design parameters, providing meaningful methods for selecting the best configuration, based on the performance parameters and the preferences of the decision maker.

The present work aims to further analyze hybrid CSP + PV plants, and determine the aforementioned trade off, through the implementation of a multi-objective optimization procedure for designing hybrid CSP + PV plants. The usefulness of such approach is addressed by analyzing two type of CSP systems parabolic trough collectors (PTC) and a central receiver system (CRS). The case study analyzed herein considers the irradiation data from Crucero in northern Chile, considered as one of the most interesting sites for deploying solar energy technologies in Chile, due to its high irradiation levels (3389 $kWh/(m^2year)$) and proximity to mining facilities that can act as demand centers [18]. In fact, it is located at short distance from the site where the Cerro Dominador project is being constructed, a CSP + PV hybrid plant featured by a 110 MW molten salt tower, and a 100 MW PV plant [19]. Regarding the multi-objective optimization procedure, three objective functions are considered: the Levelized Cost of Energy (LCOE), total investment and capacity factor. In a first approach, the LCOE and capacity factor are simultaneously optimized, and in a second stage the three objective functions are optimized, yielding a two and three-dimensions Pareto frontier, respectively. Owe to the large variation on the costs reported for each component, different scenarios of PV installed cost were considered (1.3, 1.5 and 1.9 $US\$/W_{DC}$).

Hence, the present work describes the development of an evaluation tool that allows to assess the trade off between the costs of the hybrid plant (LCOE and total cost) and its capacity factor. The methodology consists of using a combination of tools for the optimization scheme. The energy and economic assessment of the CSP plant are evaluated using TRNSYS [20] energy simulation software, coupled to GenOpt [21] to automatically run different scenarios. Optimization procedures are performed in MATLAB environment [22], which allows for a fast and efficient method of multi-objective optimization when using a sort of approximation for the fitness function (performance calculations) [23]. In addition, since selecting a solution from the set formed by the Pareto-

Frontier is dependent on the preferences and criteria of the decision maker, an example of the decision-making process is presented, considering the linear programming technique for multidimensional analysis of preference (LINMAP) [24,25].

2. System description

To analyze the effect of plant configuration on the LCOE, two CSP systems were considered: a hybrid scheme composed of a parabolic trough plant (PTC) and a PV field; and a central receiver system (CRS) coupled to a fixed PV field, as illustrated in Fig. 1. The PTC plant (Fig. 1a) consist of a standard parabolic trough field [26], operating with thermal oil as heat transfer fluid, and an indirect two tank molten sat thermal storage. The power block consist of a steam Rankine cycle, which operates at middle range temperatures (380 °C), due to the limitations of the thermal oil [26]. The CRS plant (Fig. 1b) consist of a standard solar tower plant with a circular external receiver operating with molten salt as heat transfer fluid. Because the heat transfer fluid and thermal storage media are the same, a direct two tank thermal storage is considered. Since the molten salts can operate up to 575 °C, the steam Rankine cycle of the CRS system operates at higher temperature and efficiency than the PTC plant, as described in Ref. [27].

For both schemes analyzed herein, the hypothesis is that the CSP plant dispatch responds to the PV output. That approach enables a lower-cost solution, for a specific design capacity factor, than developed by a stand-alone CSP plant. Therefore, such schemes allows to configure a power plant with a high capacity factor, without representing a significant increase on costs.

Fig. 2 depicts the operation considered in the current analysis. As observed, the PV power output increases as the CSP power output decreases during sunshine hours, keeping the CSP + PV power production almost constant and equivalent to a base-load power profile. As the CSP power output decreases, the energy absorbed by the CSP field is directed to the thermal storage. Thus, in low irradiation periods (e.g. at night) that stored energy is converted to electricity and dispatched to the grid. When the thermal storage is fully charged, part of solar field should be defocused, in order to dump the surplus of heat.

3. Methodology

The methodology used in the present study consists of a combination of tools, where TRNSYS and GenOpt are used to design the

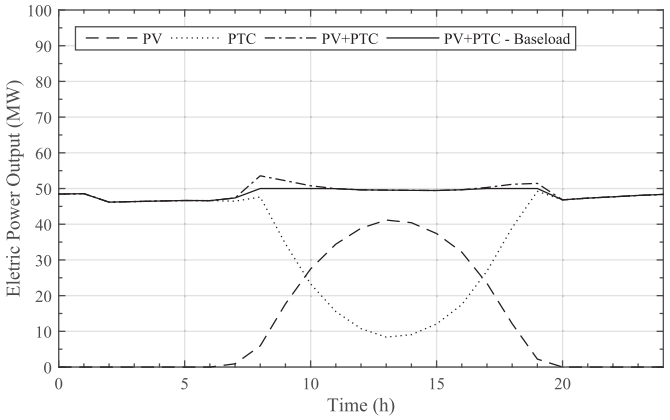

Fig. 2. Dispatch modes of power production of the CSP + PV hybrid plant at baseload production.

numerical experiments and build a performance database for each configuration. Then, the MATLAB environment is employed to read these databases, build a surrogate model and perform the optimization routine using a genetic algorithm.

TRNSYS [20] is used to assess the thermal and economic performance of each plant by means of an annual simulation, considering a transient model and using a time step of 1 h. GenOpt is used to automate the TRNSYS runs and generate a performance database, due to its easiness for configuring automate runs when combined with TRNSYS. Such configuration allows to vary the independent variables, generate the input files, run TRNSYS, and save the results in a simple process. Although GenOpt is an optimization program, it is not capable of directly handling a multi-objective optimization. Therefore, MATLAB environment is used to aggregate the performance and economic database for each plant, where the three objective functions are assessed (LCOE, total investment and capacity factor). Then, a surrogate model (e.g., response surface approximation model) is built for each of these objective functions, and a genetic algorithm (GA) is applied to solve the optimization model. This approach is a very efficient method for reducing the intrinsic computational time of GA and complex thermal system simulations [14].

There are several methods to create surrogate models (i.e., polynomial, kriging, neural networks, and support vector machines). However, there is no common opinion as to which method

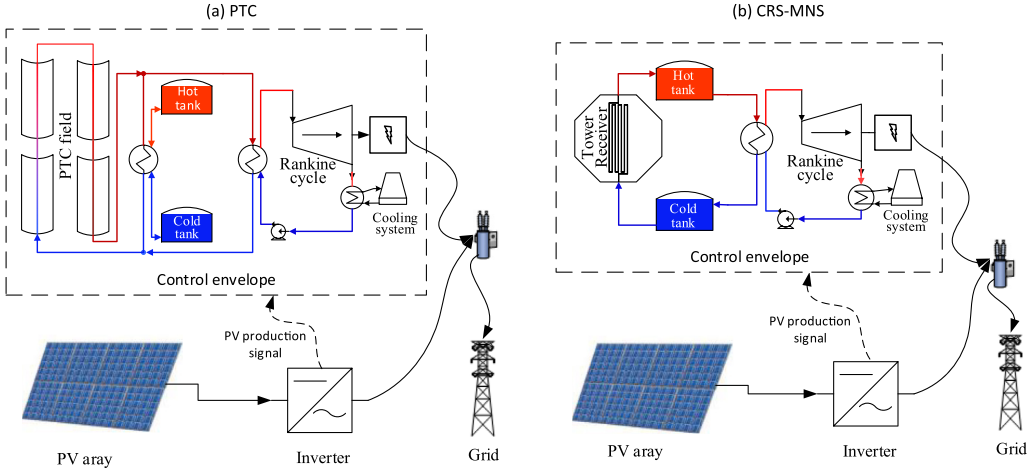

Fig. 1. CSP + PV plants configurations: parabolic trough collectors (a) and central receiver system (b).

performs better than the others, since the performance of the approximation depends on the nature of the problem addressed and more than one performance measurement can be considered [23]. In the present study, a linear interpolation method (without extrapolation) was chosen to avoid local minimums in the approximate model, as suggested in Ref. [23]. Using such method the surrogate models were built, configuring objective functions in the form $v = F(x_1, x_2, x_3, x_4)$. To ensure a good approximation within the interpolation method, for each configuration and PV cost scenario, 30976 numerical cases were evaluated in TRNSYS, which are equally spaced within the analyzed domain ($16 \times 16 \times 11 \times 11$). The total number of evaluations (185856—three cost cases for two plants; 6×30976) took almost 45 days in an 8 core processor working with eight simultaneous threads. However, this value is significantly smaller than the total fitness evaluations used by the GA algorithm, which points out the importance of using a surrogate model.

Regarding the annual performance of the hybrid plant, it was estimated using the methodology described in Ref. [12]. This simulation models use a new TRNSYS library adapted from the open access mathematical models [26–29], of the System Advisor Model (SAM) [30]. Each hybrid scheme (PTC + PV and CRS + PV) is simulated in a unique TRNSYS deck, where CSP dispatch is controlled as a response to the output from the PV array; delivering a base-load output, composed of the CSP and PV production. This coupling scheme is accomplished at each time step of the simulation by modifying the turbine output fraction, which is calculated as a function of the PV power generation. It is worth mentioning that the standard mathematical models used in NREL system advisor model (SAM), a widespread software used for simulating CSP plants, do not allow this approach.

3.1. Objective functions

The aim of hybridizing CSP plants is mainly to reduce costs (either operational or installation costs) and achieve a higher capacity factor, thus increasing the competitiveness of solar electricity. In this context, the optimization procedure for the CSP + PV hybrid plants proposed herein considers three objective functions: levelized cost of electricity, capacity factor, and initial investment.

3.1.1. Levelized cost of energy

The Levelized Cost of Electricity (LCOE) is used as a figure of merit to address the economic performance of the configuration. The LCOE is commonly used as a measure for comparing different power sources for electricity generation. It is an economic assessment of the average total cost to build and operate a power-generating asset over its lifetime per unit of energy delivered. The following definition adopted, as described in Refs. [31,32],

$$LCOE = \frac{I_0 + \sum_{t=1}^{n} \left(A_t \Big/ (1+i)^t \right)}{\sum_{t=1}^{n} W_{t,ele} \Big/ (1+i)^t} \tag{1}$$

where I_0 is the initial investment, including both the PV and the CSP costs. A_t is the annual cost considering *O&M* and insurance; and i is the discount rate. $W_{t,el}$ is the annual electricity delivered by the system, which for the hybrid CSP + PV system is defined as the baseload electricity (fixed at the nameplate capacity of the CSP plant).

3.1.2. Capacity factor

The capacity factor is a parameter commonly used for assessing power plants ability for dispatching electricity or its availability. It is defined as the ratio between the actual electricity output over a given period of time, and the maximum possible electrical energy output over the same amount of time. Hence, in an annual basis, the capacity factor for the hybrid plant is expressed as follows,

$$CF = \frac{W_{ele}}{8760 \times nameplate} \tag{2}$$

where the subscript *nameplate* represents the net nominal capacity of the hybrid plant, which is the base-load capacity that the plant is able to dispatch.

3.1.3. Total initial investment

Differently from non-renewable power plants, the initial investments of CSP plants dominates the LCOE, accounting for approximately four-fifths of the total cost [31]. Hence, LCOE has a clear trade-off with the initial investment and capacity factor; in contrast, the initial investment presents a linear relation with capacity factor. Therefore, it results interesting to assess the effect of the initial investment on the behavior of the other two parameters optimized. Including such objective function allows decision makers to select the optimal solution, based on the commitment on achieving high capacity factor, the willingness to invest or the availability of financial opportunities for the project. The total initial investment per capacity is expressed as,

$$C'_{total} = \frac{I_0}{W_{ref}} \tag{3}$$

where I_0 is the total initial investment for the hybrid plant, considering total direct costs and total indirect costs for CSP and PV components of the plant. Total direct costs consist of site preparation, solar field equipment, heat transfer fluid, thermal energy storage, power block, balance of the plant and contingency. Indirect costs account for the land cost, EPC (Engineering, Procurement, Construction), and sale taxes. W_{ref} is the gross power output of the hybrid plant, in this case 50 MW.

3.2. Decision variables

As mentioned earlier, the design parameters that present major effects on the objective functions are the size of the solar field (solar multiple (SM)), thermal storage capacity (TES_h), PV tilt angle (β) and the PV power ratio (PV_{pr}), defined as the ratio between PV installed capacity and CSP nameplate capacity. These four variable are considered as the decision space $\vec{x} = (SM, TES_h, \beta, PV_{pr})^T$, which are subjected to variable constrains, and delimit the search domain by its lower (x_i^L) and upper (x_i^U) values. The limits of the decision variables are listed in Table 1.

3.3. Optimization framework

As mentioned before, the optimization framework of this study consists of several steps. First, a database of cases is developed using the simulated data from TRNSYS and GenOpt, which consists in performance maps for each plant configuration and PV cost scenario, generated as a function of the decision variables. Then, a

Table 1
Decision variables limits (Optimization Constraints).

Variable	Lower value (x_i^L)	Upper value (x_i^U)
Solar multiple, $SM(-)$	1	4
Thermal storage, TES_h(h)	0	21
PV tilt angle, β (deg)	0	60
PV power ratio, $PV_{pr}(-)$	0	2

surrogate model is created for each of these cases in MATLAB, and finally, a Pareto frontier is determined using multi-objective genetic algorithm, which allows handling search domains with high discontinuities and non-linearities.

3.3.1. Surrogate model and validation

The first step to create the surrogate model is generating a performance map, through a parametric analysis. For each plant configuration and PV cost scenario, an equally spaced mesh was applied to create a decision variable space, in terms of the variables presented in Table 1. The performance map is delimited by the constrains in Table 1, consisting in 30976 TRNSYS evaluations, counting 16 numeric values for solar multiple 16 numeric values of equivalent hours full-load thermal storage, 11 numeric values of PV tilt angle, and 11 numeric values of PV power ratio.

The input data was used to build a performance database, and then create the surrogate model for each objective function. Since the performance map was created with a considerably large amount of data, it is possible to use an interpolation tool, rather than a polynomial function usually employed for surface methods. The Matlab *griddedInterpolant* class was used to create an interpolant surfaces ($v = F(x_1, x_2, x_3, x_4)$), which is commonly used in the optimization algorithms to calculate the fitness evaluation at any query point (xq_1, xq_2, xq_3, xq_4). The interpolated value at a query point is based on a linear interpolation of the values at neighboring grid points in each respective dimension and no extrapolation is allowed.

In order to validate the surrogate model, a sample of 3097 cases, different of the original and randomly selected from the 4-D decision space, was analyzed. These new cases were simulated using TRNSYS software and the surrogate model. The dispersion between the simulated results and the values predicted by the interpolation models for the PTC plant are illustrated in Fig. 3, showing the predicted values within ±3%, featuring a good agreement between the simulation and approximation model. The Mean Absolute Percentage Error (MAPE) for approximation models was considered acceptable, since it shows 0.5% for LCOE, 0.3% for the capacity factor, and 0.2% for the initial investment. Furthermore, the three models presented coefficient of determination R^2 close to 0.997. Similar results were observed for the simulation model of a CRS system and different PV cost scenarios.

3.3.2. Optimization method

Energy, economic and environmental modeling of thermal systems usually leads to non-linear, or mixed integer non-linear (MINLP) optimization problems [25]. Objective functions that involves solving a system of partial and ordinary differential equations, coupled to algebraic equations, in general are solved through an approximating function, since the system cannot achieve an exact solution, or it results expensive in terms of computational resources. Because of the precision of numerical solvers, a perturbation on the independent variables causes a change in the sequence of solver iterations, which causes discontinuities on the objective function; and consequently, not continuously differentiable [21]. That singularity is commonly observed when the objective function is evaluated through a numeric simulation program, such as TRNSYS. Based on that, it is crucial to consider an optimization algorithm suitable to problems where traditional optimization techniques break down, due to the irregular structure of the search domain (*i.e.* absence of gradient information). For the case of multi-objective optimization, it is required an algorithm that yields Pareto optimal points independent of function's continuity or domain convexity. Among the methods available for Multi-objective optimization metaheuristics methods allows to handle "hard optimization" problems and dealing with high discontinuities and non-linearities [33]. In that regard, Multi-objective Evolutionary Algorithms (MOEA), which include the Genetic Algorithm (GA), have been extensively employed for such purposes [13–15,25,34]. A Genetic Algorithm applies an iterative stochastic search strategy to find an optimal solution, imitating simplified principles of biological evolution. Genetic Algorithms are

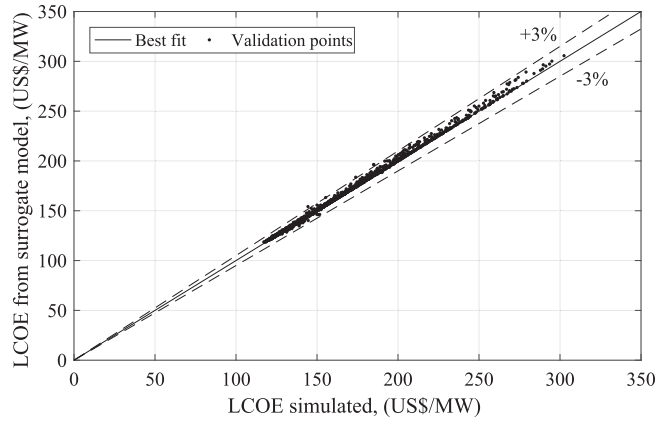

(a) LCOE

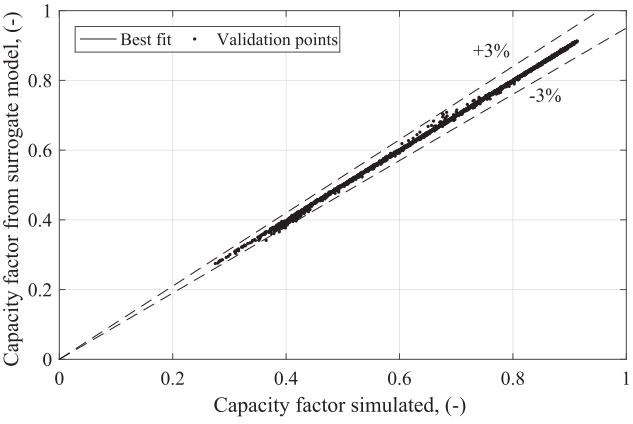

(b) Capacity factor

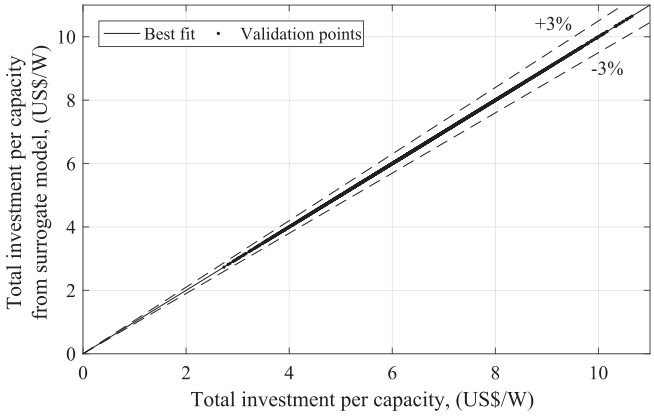

(c) Total initial investment

Fig. 3. Dispersion diagrams of the surrogate models for the PTC plant with a PV cost of 1.3 US$/Wdc.

a robust and flexible approach that can be applied to a wide range of learning and optimization problems [15,35], and therefore extensively used for optimization of thermal systems.

For purpose of the analysis described herein, the Matlab solver *gamultiobj* [22] was adopted, which considers a controlled elitist genetic algorithm (a variant of NSGA-II [36]). Furthermore, a hybrid scheme is also applied, so *gamultiobj* runs with a small number of generations to get near an optimum front; and then the solution is used as an initial point for a second optimization procedure, using *fgoalattain* (solver for goal attainment problems). Using the hybrid approach improves the effectiveness of finding an optimal Pareto front, however it compromises the diversity of the solution. This drawback can be overcome by running a second stage of *gamultiobj* using the final population returned during the last run, disregarding the hybrid procedure. The optimization algorithm runs considering the parameters listed in Table 2.

It is worth mentioning that, in order to reduce the chance of obtaining a local minimum, the tolerance, generation number and population size were enhanced with respect to the recommendations in Ref. [22]. Particular emphasis was devoted to the population size, which specify the number of design point simultaneous assessed in each iteration, therefore, searching the solution space more thoroughly. The recommended number for less than five decision variables is 200, however optimizations runs were performed ranging the Population size from 100 to 3000, without significant changes in the results. Therefore, a value of 500 was considered, because a significant reduction in the computation time was observed, with no change in the results.

3.3.3. Two objectives

In a first approach, the optimization problem was formulated considering the LCOE and capacity factor as objective functions, stated in a form that allows both objectives functions to be minimized, expressed as follows,

$$\begin{aligned} &\text{Minimize}: \begin{cases} F_1(\vec{x}) = LCOE(\vec{x}), \\ F_2(\vec{x}) = -\text{CF}(\vec{x}), \end{cases} \\ &\text{Subject to}: \\ &x_i^L <= x_i <= x_i^U, \quad i = 1,2,3,4. \end{aligned} \tag{4}$$

where F_1 and F_2 are the two objective functions, and $\vec{x}$ is a vector of independent variables: $\vec{x} = (SM, TES_h, \beta, PV_{pr})^T$. It is observed that the optimization problem is only subject to variable constrains, which delimits the decision space ($\vec{x}$) by its lower (x_i^L) and upper (x_i^U) values. A first optimization process was carried out considering the optimization problem described by Equation (4). The results for PTC collectors and a PV cost scenario of 1.3US$/$W_{DC}$ are depicted in Fig. 4. This results show the Pareto front and the feasible performance space, indicating that the optimization algorithm results in an accurate prediction of the Pareto frontier.

3.3.4. Three objectives

The second analysis the optimization problem considered three objective functions, accounting the LCOE, capacity factor and total initial investment as objectives. Similarly to the analysis described in the previous section, this optimization problem was formulated in such form that all objective functions could be minimized, as follows,

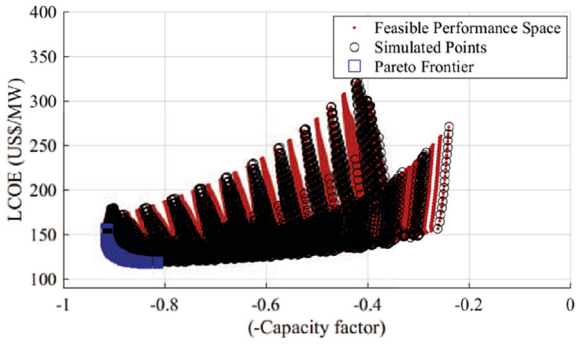

Fig. 4. Feasible performance space and the 2D Pareto front obtained from GA, for the PTC plant with a PV cost of 1.3 US$/Wdc.

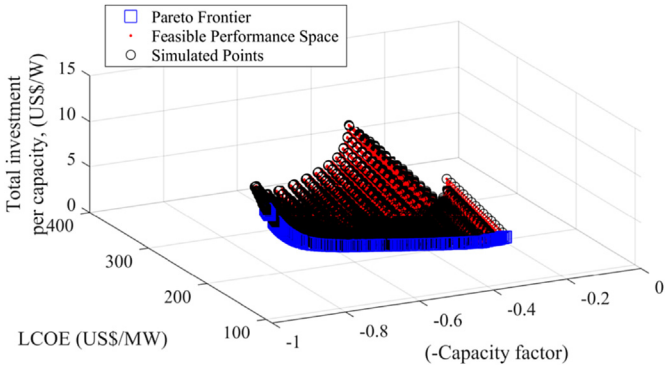

Fig. 5. Feasible performance space and the 3D Pareto front obtained from GA, for the PTC plant with a PV cost of 1.3 US$/Wdc.

$$\begin{aligned} &\text{Minimize}: \begin{cases} F_1(\vec{x}) = LCOE(\vec{x}), \\ F_2(\vec{x}) = -\text{CF}(\vec{x}), \\ F_3(\vec{x}) = C'_{total}(\vec{x}), \end{cases} \\ &\text{Subject to}: \\ &x_i^L <= x_i <= x_i^U, \quad i = 1,2,3,4. \end{aligned} \tag{5}$$

where F_1, F_2 and F_3 are the three objective functions. A second optimization procedure was carried out considering the three objective functions described above. Its results are depicted in Fig. 5, where PTC technology is considered and a PV cost scenario of 1.3US$/$W_{DC}$. It is worth mentioning that since the three objectives were not completely independent, (e.g. LCOE depends of the initial investment), the 3D Pareto front becomes a 3D curve, rather than a 3D surface. Hence, Fig. 5 shows a 3-D Pareto front and the feasible performance space.

Table 2
Genetic algorithm parameters.

Population size	Pareto fraction	Hybrid function	Tolerance	Max Stall Generations	Max Generation
500	1.0	*fgoalattain*	1×10^{-6}	3000	10000

4. Simulation parameters

4.1. Weather data

The data used in this study are hourly averages of direct measurements of DNI taken in the vicinity of Crucero with a Rotating ShadowBand Irradiometer, model RSBR2x, manufactured by Irradiance, Inc. It is a large desert plain located in extremely arid conditions, considered one of the sites of most interest for deploying solar energy technologies in northern Chile, due to its high solar resource and the ease of connecting to the grid. Most of northern Chile shares the high radiation endowment of Crucero [18]. This location has been selected as representative of the climatic conditions, and as a place of relevance in terms of energy demand for the mining industry. The main characteristics of this location are summarized in Table 3.

The design point regarding DNI for the plants simulated in this study was defined as the irradiance equivalent to 90% of the cumulative distribution function (CDF), considering the nonzero values of DNI weighted by the cosine of the incident angle. This means that for 90% of the insolation time, a value of DNI lower than 1027 W/m^2 should reach the collector mirror.

4.2. CSP and PV parameters

For both CSP systems, a power block of 50 MW of gross electric power was considered, owing to its significance in the CSP market. The configuration of the PTC plant is analogous to that observed in an actual plant located in South Spain, Andasol 1 [38]. Hence, the model considers EuroTrough ET150 solar collectors and UVA3 Schott PTR70 receivers. Additionally, the heat transfer fluid Therminol VP-1 is considered, where the design temperature is approximately 393 °C. The rated efficiency of the Rankine cycle is 38.1%, and the design cycle pressure is 100 bar.

The CRS plant is considered analogous features of Gemasolar project, also located in Spain [39]. Therefore, the model considers an external receiver and SENER heliostats (10.9×10.9 m). Moreover, the plant is modeled operating with molten salt as a heat transfer fluid and storage media, stating a design temperature of 565 °C. The rated efficiency of the Rankine cycle is 41.2%, whereas the rated cycle pressure is also 100 bar.

In addition, a molten salt mixture of 60% $NaNO_3$ - 40% KNO_3 was considered as storage media for the two-tank indirect thermal storage of the PTC plant, whereas the CRS plant uses the same salt mixture. Finally, in order to address a suitable solution for Chilean desert conditions, both plant configuration were simulated considering a dry cooling system.

The CSP plants were simulated coupled, in parallel, with a fixed PV field. To address the performance of the field in actual conditions, the performance data of actual modules was considered. In that context, the Sun Power 128-Cell Module and the Siemens SINVERT PVS1401 inverter [40] were adopted. The effect of the total capacity of the PV array on the LCOE of the hybrid plant is investigated by scaling the rated PV capacity with respect to the gross output of the CSP cycle. This procedure allows to the properly size the PV field; and show the existence of an optimal hybrid capacity, as evidenced in the following sections.

Table 3
Main characteristics of Crucero, Chile.

Parameter	Values
Latitude (°)	22.24 S
Longitude (°)	69.51 W
Altitude (m.a.s.l.)	1146
Design point DNI (irradiance, W/m^2)	1027
Yearly total for DNI (kWh/m^2year)	3389
Yearly total for GHI (kWh/m^2year)	2541
Solar database source	[37]

Table 4
Economic parameters considered for the PTC plant.

Direct costs	
Site improvements (US$/$m^2$)	15
Solar field (US$/$m^2$)	270
Heat transfer fluid (US$/$m^2$)	80
TES (US$/$kW_{th}$)	30
Fossil backup (US$/$kW_{el}$)	0
Power block (US$/$kW_{el}$)	850
Balance of plant (US$/$kW_{el}$)	105
Contingency (as % total equipment cost)	5
Indirect Costs	
Land cost (US$/acre)	0
EPC and owner cost (as % of direct cost)	11
Sales tax (%)	0
Operation and maintenance	
O&M fixed (US$/$kWh_{el}$/year of a nameplate power)	65
O&M variable (US$/$MWh_{el}$ of the annual electrical output)	3
Est. gross to net conv. factor (%)	90

4.3. Economic considerations

The main economic parameters used to evaluate the performance of hybrid plants are based on those described in Ref. [12]. Table 4 list the parameters for the PTC plant, which is based on the information reported in Ref. [38]. These values are consistent with information informed in Ref. [41], as estimated costs for 2015. The exception is the cost for the indirect 2-tank TES, which cost was adopted based on the information reported in Ref. [42]. Based on that, the TES cost varies significantly, and is influenced by the design parameters. For instance, a TES capacity of 2 h presents a cost of US$80/($kWh_{th}$); and a 12 h system has a cost of US$30/(kW h_{th}). Since the CSP + PV hybrid plants need a large storage system in order to ensure continuous base-load production, the cost of the large system was adopted (US$30/(kw h_{th})). The main economic parameters of the CRS plant are listed in Table 5,

Table 5
Economic parameters considered for the CRS plant.

Direct cost	
Site improvements (*US*$/$m^2$)	15
Solar field (*US*$/$m^2$)	180
Heat transfer fluid (*US*$/$m^2$)	0
TES (US$/$kW_{th}$)	30
Fossil backup (US$/$kW_{el}$)	0
Power block, (US$/$kW_{el}$)	1200
Balance of plant, (US$/$kW_{el}$)	350
Fixed tower cost, (MioUS$)	3
Tower scaling factor, (−)	0.0113
Receiver reference cost, (MioUS$)	110
Receiver reference area, (m)	1571
Receiver scaling factor, (−)	0.7
Contingency (as % total equipment cost)	5
Indirect Cost	
Land cost (US$/acre)	0
EPC and owner cost (as % of direct cost)	11
Sale tax (%)	0
Operation and maintenance	
O&M fixed (US$/$kWh_{el}$/year of a nameplate power)	65
O&M variable (US$/$MWh_{el}$ of the annual electrical output)	3
Estimated gross to net conversion factor (%)	90

which are based on the information reported in Ref. [43], and in agreement with the current baseline stated in Ref. [44]. The discount rate is assumed as 10%, according to current Chilean legislation. Finally, the project lifetime was established at 25 years, and no subsidies were considered, because such incentives do not exist in Chile for CSP projects.

For the PV system, owe to the large variation in the costs reported for each component, different scenarios of total installed cost per capacity were considered (1.3; 1.5 and 1.9 US$/W(dc)) [45,46]. In addition, a cost of 20 US$/kW/year was adopted regarding the O&M costs of the PV system, and an annual insurance rate of 0.5% of the total cost [45].

The cost values for the tower and receiver were scaled according to the equations described in Ref. [47]:

$$C_{tower} = C_{tower,f} \exp\left[\chi_{tower}\left(h_{tower} - \frac{h_{rec}}{2} + \frac{h_h}{2}\right)\right] \quad (6)$$

$$C_{rec} = C_{rec,ref}\left(\frac{A_{rec}}{A_{rec,ref}}\right)^{\chi_{rec}} \quad (7)$$

where the scaling factor (χ) used in Equation (6) and Equation (7) is presented in Table 5. The variables h_{tower}, h_{rec} and h_h are the heights of the tower, receiver and heliostat, respectively; and A_{rec} is the actual area of the receiver. These four quantities are calculated by the DELSOL3 code [48]. The power block and balance of plant costs listed in Tables 4 and 5 are scaled to the power block size considered in this study, as describes the following equation [49]:

$$C_{PB,BP} = Ce_{PB,BP} P_{B,ref}\left(\frac{P_{PB}}{P_{PB,ref}}\right)^{\chi_{PB,BP}} \quad (8)$$

where P_{PB} is the actual capacity of the power block, and the scaling factor ($\chi_{PB,BP}$) for the power block and balance of plant was assumed as 0.7, as suggested in Ref. [45]. The specific costs ($Ce_{PB,BP}$) are listed in Tables 4 and 5, while the reference sizes for the power block ($P_{PB,ref}$) are those reported in Refs. [38,43], 50 and 115 MW for the PTC and CRS plants, respectively.

5. Results

5.1. Two objectives functions

Fig. 6 depicts the Pareto frontiers derived from the two objectives ($LCOE - CF$) optimization process, for the three PV costs scenarios and the different technologies analyzed. The illustration clearly shows the trade-off between the two objectives, configuring the negotiation region. In that regard, the Pareto front aids the decision maker chose a single solution from the set of optimal solution based in the preferences for implementing a CSP + PV plant that develops larger capacity factors or lower LCOE. It is also demonstrated the effect of reducing the PV cost on the Pareto frontiers, which dislocates the curves to lower values of LCOE, without significant change on the values of the capacity factors.

The optimal solutions for PTC + PV plants (Fig. 6a) show three distinct regions, where LCOE slightly increases as the capacity factor increases up to 87.5%. A further increment on the capacity factor, from 87.7% to 91% (point B), yields a moderate increase on the LCOE, however a larger increase on the capacity factor shows a drastically increase on the LCOE. For instance, considering the PV cost scenario of 1.3US$/$W_{DC}$, the first region (capacity factor up to 87.5%) shows a variation on the LCOE between 118US$/MWh and 121US$/MWh. For the region with moderate change in the LCOE, it

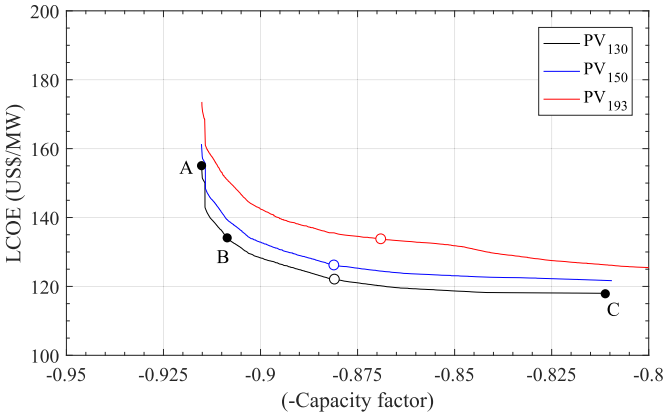

(a) PTC

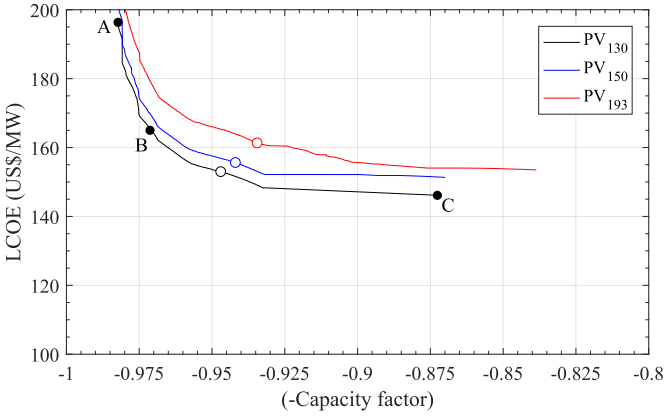

(b) CRS-MNS

Fig. 6. Two objectives Pareto optimal frontiers. Optimal design selected by LINMAP decision maker is highlighted.

ranges from 121US$/MWh to 136US$/MWh, and the last region shows an increment on the LCOE from 136US$/MWh to 155US$/MWh. It is shown in Fig. 6a that also for a PV cost of 1.3US$/$W_{DC}$ the maximum capacity factor exist at point A (91.5%), associated to the higher LCOE (155 US$/MWh). The minimum LCOE occurs on point C (118 US$/MWh), with a capacity factor of 81%. It is worth mentioning that design point A is the optimal solution when the capacity factor is the only objective function, while design point C is the optimal condition for a single optimization of the LCOE. It is also observed in Fig. 6a that the difference between the capacity factors at point A and B is not significant, while the difference on cost is relevant. Therefore, the region considered for design is between points C to B, where the changes in the LCOE are not expressive. This regions constitutes the negotiation, region where the decision-makers can chose one of the optimal solutions depending on specific preferences and criteria.

To assist the optimal design of the PTC + PV plant, the following expression can be used for a PV cost of 1.3US$/$W_{DC}$, which is derived from region C to B of the Pareto optimal curve, and is valid for capacity factor between 0.81 and 0.91,

$$LCOE = 1342CF^{45.98} + 118.1 \quad (9)$$

Similarly, for the CRS + PV plant (Fig. 6b) it is observed a three regions on the Pareto front. A first region where the LCOE slightly increases as the capacity factor increases up to 93.5%. Varying the capacity factor from 93.5% to 97% (point B) generates a moderate

increment on the LCOE, while a further increase on the capacity factor shows a substantial gain on the LCOE. Again, considering the PV cost scenario of 1.3US$/$W_{DC}$ as example, the first region (capacity factor up to 93.5%) shows a variation on LCOE from 146.2US$/MWh to 148.1US$/MWh. A moderate change region is configured, where the LCOE changes from 148.1US$/MWh to 163.9US$/MWh, and in the last region the LCOE increases from 163.9US$/MWh to 196US$/MWh. The points A and C are the design point when the maximization of capacity factor and minimization of LCOE are considered as single objective functions. The maximum capacity factor exist at point A (98.2%), associated to the higher value of LCOE (196US$/MWh). While the minimum LCOE occurs on point C (146.2US$/MWh), with a capacity factor of 87%. Similar to the PTC + PV results, the negotiation region is between points C to B, where the changes on the LCOE are not expressive.

To assist the optimal design of the PTC + PV plant, the following expression can be used for a PV cost of 1.3US$/$W_{DC}$, which is derived from region C to B of the Pareto optimal curve, and is valid for capacity factor between 0.87 and 0.97,

$$LCOE = 85.95CF^{54.53} + 147.7 \tag{10}$$

These results suggest that PTC + PV plants present a more attractive LCOE, while the CRS + PV plants can achieve capacity factors of almost 100%, providing base-load electricity. However, as suggested by Starke et al. [12], increasing the size of the CRS plant allows reducing the electricity cost (i.e., economy of scale). The authors showed that increasing cycle's gross power output of the CRS + PV plant to 100 MW–150 MW, can reduce the LCOE to 140 US$/MWh and 130US$/MWh, respectively. On the other hand, for the PTC + PV plant that economy of scale is restricted.

5.2. Three objectives functions

Fig. 7 depicts the Pareto frontiers for the three objectives ($LCOE - CF - C'_{total}$) optimization process, considering the different scenarios and technologies analyzed. It is also presented the 2D planes of the 3D Pareto front for better visualization. The inclusion of the total investment as objective function provides means for decision makers to select an optimal solutions, based on their commitment for investing on the project. In addition, the analysis considering three objectives functions allows assessing a wider range of capacity factors, and therefore a wider zone of negotiation. That is particularly interesting in cases where a high capacity factor is not a project constraint. Naturally, at lower initial investment and lower capacity factor scenarios, the plant delivers less energy, presenting a larger LCOE.

It is shown in Fig. 7a, that for a PV cost scenario of 1.3US$/$W_{DC}$, that the total investment increases linearly as the capacity factor increases, up to 80%. Increasing the capacity factor from 80% to 90% (point B) results in a moderate increment on the total cost, while a further increase in the capacity factor yields a drastically increase in the total cost. Concomitant to the increase on capacity factor, the LCOE significantly decreases to 55% (point D). Increasing the capacity factor to larger values than 55%, allows reducing the LCOE to a minimum value, then, a further increase on the capacity factor yields to a sharp growth on the LCOE. The same minimum point of the LCOE is observed on the total investment versus LCOE chart. Three additional points are noticed in Fig. 7a. Design point A is the optimal solution when the capacity factor is the only objective function (91.5%), which results in a maximum LCOE (155.1US$/MWh) and maximum total investment (9.5US$/W). Design point C is the optimal solution when the minimization of LCOE is considered as a single optimization problem (128.4US$/MWh), which yields a capacity factor of 90% and an initial investment of 7.63US$/W. Finally, design point E is the optimal solution when the initial investment is the priority (2.45US$/W considering the design parameters constrains), which also results in a low capacity factor (26.4%) and a higher LCOE (155US$/MWh). Based on the relations between capacity factor, initial cost and LCOE it is possible to establish that the useful region is between points B and D, where the changes on the capacity factor do not present significant variation on the LCOE and the Initial cost. Within this region the capacity factor varies between 90% and 55%, while the LCOE ranges from 128.4US$/MWh to 126.9US$/MWh, and the initial cost varies between 7.63US$/W and 4.45US$/W.

To assist the optimal design of the CSP + PV plant, a parametric equation (LCOE and C'_{total} as a function of capacity factor) can be used for a PV cost of 1.3US$/$W_{DC}$, which is derived from region D to B of the Pareto optimal curve, valid for a capacity factor between 0.55 and 0.9,

$$\begin{aligned} LCOE &= \frac{82158.4CF^4 - 639635.9CF^3 + 2277603.2CF^2 - 2820333.2CF + 1106299.0}{CF^3 + 8487.3CF^2 - 15564.8CF + 7136.5} \\ C'_{total} &= \frac{-3.221CF^4 + 16.36CF^3 - 22.38CF^2 + 9.596CF - 0.3191}{CF^2 - 1.844CF + 0.8504} \end{aligned} \tag{11}$$

For the hybrid CRS + PV plant (Fig. 7b), considering also the PV cost scenario of 1.3US$/$W_{DC}$, it is observed a similar behavior. However it shows slightly higher cost and capacity factors. Design point A (capacity factor as only objective) results in a maximum capacity factor of 98.3% with a LCOE of 197.5US$/MWh and initial investment of 12.64US$/W. The minimum LCOE is observed in point C (LCOE as sole objective), with a value of 148.3US$/MWh, a capacity factor of 92.2% and initial investment of 8.68US$/W. In turn, design point E (only the initial investment per capacity as objective) yields a minimum initial investment of 4.18US$/W, with a capacity factor of 29.1% and LCOE of 240.8US$/MWh. Additionally, considering the region with moderate variation in the LCOE and initial cost, is possible to define two additional relevant points: B and C, with a capacity factor of 97% and 63%, respectively. The space between B and D constitutes the negotiation region, where the LCOE varies from 165.2US$/MWh to 166US$/MWh, passing trough a minimum point of 148.3US$/MWh, and the initial cost varies from 10.31US$/W to 6.495US$/W. Within the negotiation region, the changes on the LCOE are nor expressive, so decision makers can rank the optimal solutions according specific criteria.

Similar to the configurations described above, the following equation can be used to assist the optimal design of the CRS + PV plant, which is derived from region D – B of the Pareto set, valid for capacity factor between to 0.63 and 0.97,

$$LCOE = \frac{3143543.5CF^4 - 11300842.0CF^3 + 17059187.6CF^2 - 13021965.2CF + 4127027.1}{CF^3 + 10257.6CF^2 - 22573.8CF + 12339.8}$$
$$C'_{total} = \frac{9418.3CF^4 - 23692.8CF^3 + 23626.8CF^2 - 15258.3CF + 5940.5}{CF^3 + 879.7CF^2 - 1956.8CF + 1077.7} \quad (12)$$

5.3. Final optimal solution through decision-making process

To fully demonstrate the usefulness of the optimization process, a decision-making method was applied to select the final optimal solution from the Pareto frontiers. Such method is required since the dimensions of objective functions are different, and it should be unified. In this study, the Linear Programming Technique for Multidimensional Analysis of Preference (LINMAP) developed by Srinivasan and Shocker [24] was adopted. In this approach, each objective function is subjected to a Euclidian non-dimensionalization [25], defined as follows,

$$F_{ij}^n = \frac{F_{ij}}{\sqrt[2]{\sum_{j=1}^{m} (F_{ij})^2}} \quad (13)$$

where F_{ij}^n is the "i" nondimensionalized objective, and F_{ij} denotes the "j" points of the "i" objective on the Pareto frontier.

After the nondimensionalization procedure of the objective functions, the LINMAP method is applied, consisting of calculating the spacial distance between each point from the Pareto frontier and an ideal point, as follows,

$$d_j = \sqrt[2]{\sum_{i=1}^{n} \left(F_{ij} - F_i^{Ideal}\right)^2} \quad (14)$$

where d_j denotes the distance between the "j" point and the ideal point, while "i" stands for each objective function and n denotes the number of objectives. F_i^{Ideal} is the ideal value of the i^{th} objective, defined from the information derived from a single-objective optimization procedure. Hence, the ideal solution is the point that optimizes each objective function, disregarding the other objectives. The final optimal solution is selected as the solution presenting the minimum distance from the ideal point. Therefore, it is defined as

$$j_{final} \equiv j \in \min(d_j) \quad (15)$$

The final optimal solution for each plant is highlighted by a circular marker in Figs. 6 and 7. Table 6 shows these final optimal solutions, listing the values of the objectives functions and the design variables. From those results, it is clear that the PTC + PV plant provides the lowest LCOE, between 121 US$/MWh to 133 US$/MWh, disregarding the number of objectives considered. Meanwhile CRS + PV plants provides electricity cost between 152US$/MWh to 160US$/MWh. For the two objectives case, the capacity factor of the PTC + PV is around 88%, while the capacity factor of the CRS + PV arises close to 94%. For the three objective case, the capacity factor values are reduced to 65% and 79% for the PTC + PV and CRS + PV, respectively. The inclusion of the initial investment as third objective, induced designing plants with lower capital costs, at the same level of LCOE, but with a significant reduction on the capacity factor.

For the two objective analysis, the differences between final optimal solutions lies on the increase of the LCOE and initial investment, due to variations on the PV costs, with a small change on the solar multiple. However, for the three objectives analysis, an increase on the PV cost reduces the advantage of hybridization, forcing a reduction on the PV power ratio, compensated by an increase on the solar multiple (keeping a constant capacity factor). This occurs since one of the objectives aims to minimize the initial investment, which increases for higher PV costs. It is also important to mention that the minimization of the initial investment should be addressed with a lower solar multiple and thermal storage. For example, the final solution of the PTC + PV plant considering a PV cost scenario of 1.3US$/W(dc) and two objectives, considering a solar multiple of 2.179 and TES hour of 14.012, while for the three objective case the final solution presents a solar multiple of 1.429 and TES hour of 9.984.

The concrete benefit of hybridization is fully demonstrated when comparing the performance of these plants against the stand-alone PTC and CRS plants. By designing an equivalent PTC plant without hybridization, optimizing only the LCOE, it is possible to achieve a LCOE of 128.4US$/MWh and a capacity factor of 80.1%, where the solar multiple is 3.3 and the TES size is 14.3 h. Similarly, for the stand-alone CRS plant a LCOE of 154.5US$/MWh and capacity factor of 85.9% are achieved, where the solar multiple and TES size are 3.0 and 15 h, respectively. Comparing these values to those presented in Table 6, results evident that the hybridization can simultaneously reduce the LCOE, increasing the capacity factor, but the most important effect is the significant reduction on the solar field size.

6. Conclusions

A methodology for rating and design CSP + PV hybrid systems has been presented, which has the potential for helping to reduce their operational and installation costs, as well as increasing the capacity factor of hybrid plants. Using a multi-objective routine, the trade off between the LCOE, initial investment and capacity factor, has been demonstrated, and then determined. Two case study were presented for demonstrating the usefulness of this methodology, namely, parabolic trough collectors (PTC) and a central receiver system (CRS), coupled to a PV array. Three objective functions were considered in the multi-objective optimization procedure: the Levelized Cost of Energy (LCOE), total investment and capacity factor. Regarding the design variables, four variables were considered, such as: the size of the solar field, thermal storage capacity, PV tilt angle and PV power ratio.

First, the LCOE and capacity factor were simultaneously optimized, yielding a clear trade-off between these two figures of merits. With this result, it was possible to identify the negotiation region. Seeking for a wide range of optimal capacity factor, the total investment was also considered as objective, which yields a three-dimensions Pareto frontier. This result provides useful insights about the trade off between these three figures of merits, and enables identifying a wider zone of negotiation. That is particularly interesting in cases where a higher capacity factor is not a project

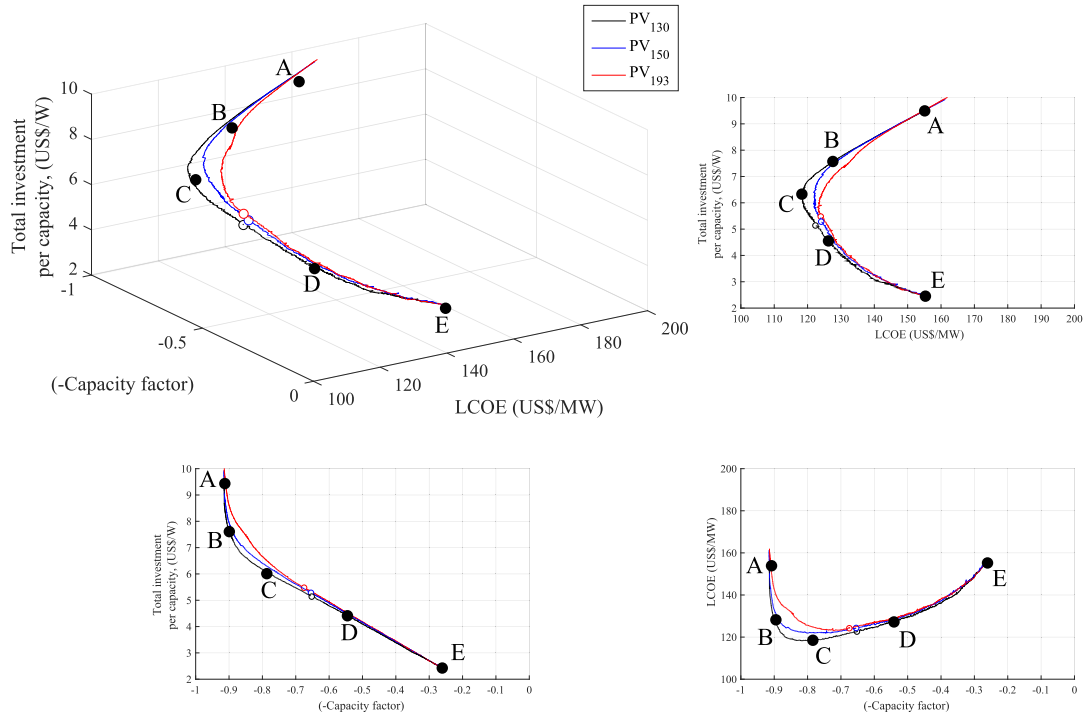

(a) PTC

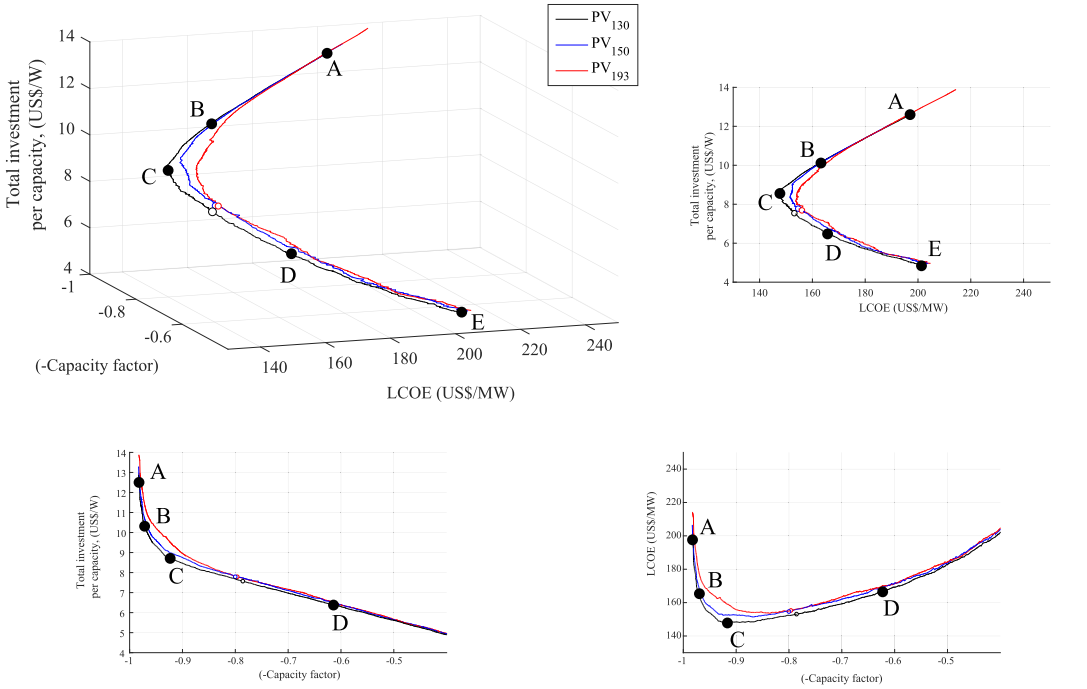

(b) CRS-MNS

Fig. 7. Three objectives Pareto optimal frontiers. Optimal design selected by LINMAP decision maker is highlighted.

constraint. Identifying such Pareto frontier, and negotiation region, also allow us derive equations for the Pareto optimal points for each objective, which are useful tools for design such plants. It is also demonstrated that reducing the PV cost dislocates the Pareto frontiers to lower values of LCOE. The results also suggest that PTC + PV plants present a more attractive LCOE, while the CRS + PV plants can achieve capacity factors of almost 100%, providing base-load electricity.

Regarding the selection of final optimal solutions, it is evident that the PTC + PV plant provides the lowest LCOE, between 121 US$/MWh and 133 US$/MWh, disregarding the number of objectives considered. Meanwhile CRS + PV plants provides electricity

Table 6
Final optimal solutions specified by LINMAP decision maker.

		PV cost $\left(\frac{US\$}{W_{dc}}\right)$	CF (−)	LCOE $\left(\frac{US\$}{MWh}\right)$	$C'_{total}\left(\frac{US\$}{W}\right)$	Solar multiple (−)	TES hour (h)	PV tilt angle (°)	PV_{pr} (−)
Two-obj.	PTC	1.30	0.880	121.677	7.074	2.179	14.012	30.107	1.404
		1.50	0.882	126.335	7.323	2.200	14.255	30.110	1.402
		1.93	0.869	133.681	7.744	2.054	14.058	29.734	1.394
	CRS-MNS	1.30	0.947	152.922	9.133	2.257	16.478	29.680	1.400
		1.50	0.943	155.870	9.419	2.169	16.770	30.181	1.400
		1.93	0.933	160.833	9.651	2.009	15.531	29.856	1.392
Three-obj.	PTC	1.30	0.648	122.690	5.112	1.429	9.984	34.606	0.975
		1.50	0.653	124.254	5.266	1.992	10.712	33.915	0.390
		1.93	0.657	124.570	5.344	2.407	11.557	15.702	0.011
	CRS-MNS	1.30	0.780	153.301	7.523	1.608	12.536	31.267	1.080
		1.50	0.796	154.763	7.756	2.588	13.732	39.766	0.069
		1.93	0.781	156.170	7.667	2.549	13.869	42.859	0.029

costs of 152 US$/MWh to 160US$/MWh. For the two objectives case, the capacity factor of the PTC + PV is around 88%, while the capacity factor of the CRS + PV arises close to 94%. For the three objective case, the capacity factor values are reduced to 65% and 79% for the PTC + PV and CRS + PV, respectively. Designing an equivalent PTC and CRS plants with no hybridization, it is possible to demonstrate the benefit of hybridization. A stand-alone PTC plant, optimizing only the LCOE, achieve a LCOE of 128.4US$/MWh and capacity factor of 80.1%, with a solar multiple and TES size of 3.3 and 14.3 h, respectively. Similarly, a stand-alone CRS plant, achieve a LCOE of 154.5US$/MWh and capacity factor of 85.9%, with a solar multiple and TES size of 3.0 and 15 h, respectively. Comparing these values to those obtained in the multi-objective optimization, evidence that the hybridization can simultaneously reduce the LCOE, increases the capacity factor, but the most important effect is the significant reduction on the solar field size.

Sizing a hybrid CSP + PV plant is a multi-objective optimization problem, featured by multiple and competing objectives with clear trade offs. These kinds of problems are difficult to solve and time consuming in terms of simulation and engineering processes. Therefore, the proposed methodology contributes to the proper assessment of such systems, through a practical and comprehensive approach, which allows to address several factors (independent variables and objectives) simultaneously. The Pareto frontiers provides useful tools to analyses the trade offs between the objectives, providing decision-making mechanisms to aid a proper design.

Acknowledgement

The authors wish to express their gratitude to CAPES (Brazilian Federal Agency for Support and Evaluation of Graduate Education) for partially funding the present work through a scholarship from Allan R. Starke. The authors also appreciate the financial support from CONICYT/FONDAP 15110019 “Solar Energy Research Center”-SERC-Chile and the project CONICYT/Fondecyt N° 11140725.

Nomenclature

A_t	Annual cost, (US$)
A_{rec}	Receiver area
CF	Capacity factor, (−)
C	Cost
C'_{total}	Initial investment per capacity, (US$/kW)
d	Distance between the Pareto frontier and Ideal point
F_1	First objective
F_2	Second objective
F_3	Third objective
F_{ij}	Value of the “j^{th}” point of the “i^{th}” objective of the Pareto frontier
h	Heights, (m)
i	Discount rate
j	Index of final solution
I_0	Initial investment of the plant, (US$)
$LCOE$	Levelized Cost of Energy, (US$/MWh)
$nameplate$	Net nominal capacity of the plant, (MW)
PV_{pr}	PV power ratio, (−)
SM	Solar multiple, (−)
TES_h	Thermal storage capacity in hours, (h)
$W_{t.ele}$	Annual electricity delivered by the plant, (MWh)
W_{ref}	Gross power output of the hybrid plant
$\vec{x}$	Decision variables space
x_i	“i^{th}” variable of the decision space

Acronyms

ANN	Artificial Neural Networks
CRS	Central Receiver System
CPV	Concentrating Photovoltaic
CSP	Concentrating Solar Power
CDF	Cumulative Distribution Function
DC	Direct Current
DNI	Direct Normal Irradiance
EPC	Engineering, Procurement, Construction
GenOpt	Generic Optimization Program
GA	Genetic Algorithm
GHI	Global Horizontal Irradiance
HRES	Hybrid Renewable Energy System
LINMAP	Linear Programming Technique for Multidimensional Analysis of Preference
MAPE	Mean Absolute Percentage Error
MINLP	Mixed Integer Non-Linear Problem
MOEA	Multi-Objective Evolutionary Algorithm
O&M	Operation and Maintenance
ORC	Organic Rankine Cycle
PV	Photovoltaic
SAM	System Advisor Model
TOPSIS	Technique for Order of Preference by Similarity to Ideal Solution
TMY	Typical Meteorological Year
TRNSYS	Transient System Simulation Program

Greek symbols

β	PV tilt angle, (deg)
χ	Scaling factor, (−)

Subscript

t	Years
BP	Balance of plant
ele	Electrical
final	Final
f	Fixed
h	Heliostat
i	Objective number
PB	Power block
rec	Receiver
ref	reference
j	Solution points
tower	Tower

Superscript

Ideal	Ideal point
L	Lower
n	Nondimensionalized
U	Upper

References

[1] WEO. World energy outlook 2016. Tech. Rep. Paris: International Energy Agency; 2016. https://doi.org/10.1787/weo-2016-en.

[2] Branz HM, Regan W, Gerst KJ, Borak JB, Santori Ea. Hybrid solar converters for maximum exergy and inexpensive dispatchable electricity. Energy Environ Sci 2015;8(11):3083–91. https://doi.org/10.1039/C5EE01998B.

[3] Denholm P, Margolis RM. Evaluating the limits of solar photovoltaics (pv) in electric power systems utilizing energy storage and other enabling technologies. Energy Pol 2007a;35(9):4424–33. https://doi.org/10.1016/j.enpol.2007.03.004.

[4] Denholm P, Margolis RM. Evaluating the limits of solar photovoltaics (pv) in traditional electric power systems. Energy Pol 2007b;35(5):2852–61. https://doi.org/10.1016/j.enpol.2006.10.014.

[5] Yang H, Lu L, Zhou W. A novel optimization sizing model for hybrid solar-wind power generation system. Sol Energy 2007;81(1):76–84. https://doi.org/10.1016/j.solener.2006.06.010.

[6] Zhou W, Lou C, Li Z, Lu L, Yang H. Current status of research on optimum sizing of stand-alone hybrid solar–wind power generation systems. Appl Energy 2010;87(2):380–9. https://doi.org/10.1016/j.apenergy.2009.08.012.

[7] IEA. Technology roadmap: solar thermal electricity. Tech. Rep. Paris, France: International Energy Agency; 2014. https://doi.org/10.1007/SpringerReference_7300.

[8] Green A, Diep C, Dunn R, Dent J. High capacity factor CSP-PV hybrid systems. Energy Procedia 2015;69:2049–59. https://doi.org/10.1016/j.egypro.2015.03.218.

[9] Platzer WJ. Combined solar thermal and photovoltaic power plants – an approach to 24h solar electricity?. In: Proceedings of SolarPACES 2015; 2016. Capetwon. South-Africa.

[10] Petrollese M, Cocco D. Optimal design of a hybrid CSP-PV plant for achieving the full dispatchability of solar energy power plants. Sol Energy 2016;137:477–89. https://doi.org/10.1016/j.solener.2016.08.027.

[11] Cocco D, Migliari L, Petrollese M. A hybrid CSP-CPV system for improving the dispatchability of solar power plants. Energy Convers Manag 2016;114:312–23. https://doi.org/10.1016/j.enconman.2016.02.015.

[12] Starke AR, Cardemil JM, Escobar RA, Colle S. Assessing the performance of hybrid CSP+PV plants in northern Chile. Sol Energy 2016;138:88–97. https://doi.org/10.1016/j.solener.2016.09.006.

[13] Lazzaretto A, Toffolo A. Energy, economy and environment as objectives in multi-criterion optimization of thermal systems design. Energy 2004;29(8):1139–57. https://doi.org/10.1016/j.energy.2004.02.022.

[14] Magnier L, Haghighat F. Multiobjective optimization of building design using TRNSYS simulations, genetic algorithm, and artificial neural network. Build Environ 2010;45(3):739–46. https://doi.org/10.1016/j.buildenv.2009.08.016.

[15] Ahmadi P, Dincer I, Rosen MA. Exergy, exergoeconomic and environmental analyses and evolutionary algorithm based multi-objective optimization of combined cycle power plants. Energy 2011;36(10):5886–98. https://doi.org/10.1016/j.energy.2011.08.034.

[16] Asadi E, da Silva MG, Antunes CH, Dias L. A multi-objective optimization model for building retrofit strategies using TRNSYS simulations, GenOpt and MATLAB. Build Environ 2012;56:370–8. https://doi.org/10.1016/j.buildenv.2012.04.005.

[17] Li Y, Liu G, Liu X, Liao S. Thermodynamic multi-objective optimization of a solar-dish Brayton system based on maximum power output, thermal efficiency and ecological performance. Renew Energy 2016;95:465–73. https://doi.org/10.1016/j.renene.2016.04.052.

[18] Escobar RA, Cortés C, Pino A, Salgado M, Pereira EB, Martins FR, et al. Estimating the potential for solar energy utilization in Chile by satellite-derived data and ground station measurements. Sol Energy 2015;121:139–51. https://doi.org/10.1016/j.solener.2015.08.034.

[19] SEA. Description of the Cerro dominador project. 2014. http://seia.sea.gob.cl/expediente/ficha/fichaPrincipal.php?modo=ficha&id_expediente=2128879352.

[20] Klein SA. TRNSYS: a transient systems simulation program. 2010., V. 17. .

[21] Wetter M. GenOpt - generic optimization program - user manual. Tech. Rep. c. Ernest Orlando Lawrence and Berkeley National Laboratory; 2008., V 2.1.0. .

[22] The MathWorks Inc. The mathworks. 2015. http://www.mathworks.com.

[23] Jin Y. A comprehensive survey of fitness approximation in evolutionary computation. Soft Computing 2005;9(1):3–12. https://doi.org/10.1007/s00500-003-0328-5.

[24] Srinivasan V, Shocker A. Linear programming techniques for multidimensional analysis of preferences. Psychometrika 1973;38(3):337–69. https://doi.org/10.1007/BF02291658.

[25] Sayyaadi H, Mehrabipour R. Efficiency enhancement of a gas turbine cycle using an optimized tubular recuperative heat exchanger. Energy 2012;38(1):362–75. https://doi.org/10.1016/j.energy.2011.11.048.

[26] Wagner MJ, Gilman P. Technical manual for the SAM physical trough model. Tech. Rep. NREL; National Renewable Energy Laboratory; 2011.

[27] Wagner MJ. Simulation and predictive performance modeling of utility-scale central receiver system power plants. Master thesis. UNIVERSITY OF WISCONSIN – MADISON; 2008.

[28] Wagner MJ, Zhu G. A direct steam linear Fresnel performance model for NREL's SAM. In: Proceedings of the ASME 2012 6th international conference on energy sustainability & 10th fuel cell science, engineering and technology conference. San Diego,CA: ASME; 2012.

[29] Neises T, Wagner MJ. Simulation of direct steam power tower concentrated solar plant. ASME 2012. In: 6th international conference on energy sustainability, parts A and B; 2012. p. 499–507. https://doi.org/10.1115/ES2012-91364.

[30] Blair N, Dobos A, Freeman J, Neises T, Wagner M, Ferguson T, et al. System advisor model. SAM 2014.1.14. 2014. http://www.nrel.gov/docs/fy14osti/61019.pdf.

[31] IRENA. Renewable energy technologies: cost analysis series - concentrating solar power. Tech. Rep. 2. International Renewable Energy Agency; 2012.

[32] Kost CMJ, Thomsen J, Hartmann N, Senkpiel C, Philipps S, Nold S, et al. Levelized cost of eletricity renewable energy technologies. Fraunhofer-ISE Study. Tech. Rep. November; Fraunhofer-ISE Study; Friburg, Germany. 2013.

[33] Collette Y, Siarry P. Multiobjective optimization: principles and case studies. In: Decision engineering. Berlin Heidelberg: Springer; 2004, ISBN 9783540401827.

[34] McCall J. Genetic algorithms for modelling and optimisation. J Comput Appl Math 2005;184(1):205–22. https://doi.org/10.1016/j.cam.2004.07.034.

[35] Arora JS. Introduction to optimum design. Academic Press; 2011, ISBN 9780123813756.

[36] Deb K, Agrawal S, Pratap A, Meyarivan T. A fast elitist non-dominated sorting genetic algorithm for multi-objective optimization: NSGA-II. In: Parallel problem solving from nature PPSN VI, 6th international conference. Paris, France. Berlin, Heidelberg: Springer; 2000, ISBN 978-3-540-41056-0. p. 849–58. https://doi.org/10.1007/3-540-45356-3_83.

[37] Escobar Ra, Cortés C, Pino A, Pereira EB, Martins FR, Cardemil JM. Solar energy resource assessment in Chile: satellite estimation and ground station measurements. Renew Energy 2014;71:324–32. https://doi.org/10.1016/j.renene.2014.05.013.

[38] NREL. System advisor model (SAM) case study: Andasol-1. 2013. https://sam.nrel.gov/sites/default/files/content/case_studies/sam_case_csp_physical_trough_andasol-1_2013-1-15.pdf.

[39] NREL. System advisor model (SAM) case study: gemasolar. 2013. https://sam.nrel.gov/sites/sam.nrel.gov/files/content/case{_}studies/sam{_}case{_}csp{_}salt{_}tower{_}gemasolar{_}2013-1-15.pdf.

[40] SAM. System advisor model version 2014.1.30. In: User documentation. Sizing the flat plate PV system; 2014.

[41] Turchi C. Parabolic Trough reference plant for cost modeling with the solar advisor model (SAM). Tech. Rep. July. Golden, Colorado: National REnewable Energy Laborattory; 2010.

[42] Kelly B, Kearney D. Thermal storage commercial plant design study for a 2-tank indirect molten salt system. Tech. Rep. July. National Renewable Energy Laboratory; 2006.

[43] Turchi CS, Heath Ga. Molten salt power tower cost model for the system advisor model (SAM). Tech. Rep. February. National Renewable Energy Laboratory; 2013.

[44] Kolb GJ, Ho CK, Mancini TR, Gary JA. Power tower technology roadmap and cost reduction plan. Tech. Rep. April. Albuquerque, New Mexico: SANDIA National Laboratories; 2011.

[45] U.S. Department of Energy. SunShot vision study: concentrating solar power: technologies, cost, and performance. Tech. Rep. February. U.S. Department of Energy; 2012.

[46] Chung D, Davidson C, Fu R, Ardani K, Margolis R. US photovoltaic prices and cost breakdowns: Q1 2015 benchmarks for residential, commercial, and utility-scale systems. Tech. Rep. September. Golden, CO (USA): National Renewable Energy Laboratory; 2015.

[47] Gilman P, Blair N, Mehos M, Christensen C, Janzou S, Cameron C. Solar advisor model: user guide for version 2.0. Tech. Rep. August. Golden, CO (USA): National Renewable Energy Laboratory; 2008. http://www.nrel.gov/docs/fy08osti/43704.pdf.

[48] Kistler BL. A User's manual for DELSOL3: a computer code for calculating the optical performance and optimal system design for solar thermal central receiver plants. Tech. Rep. Albuquerque, New Mexico: Sandia National Laboratories; 1986.

[49] Avila-Marin AL, Fernandez-Reche J, Tellez FM. Evaluation of the potential of central receiver solar power plants: configuration, optimization and trends. Appl Energy 2013;112:274–88. https://doi.org/10.1016/j.apenergy.2013.05.049.